The 7th International Supercritical CO_2 Power Cycles Symposium
February 21-24, 2022, San Antonio, Texas
Paper #39

Exploring Materials Options for Ultra-High Temperature Supercritical CO_2 Applications

Bruce A. Pint
Group Leader
Oak Ridge National Laboratory
Oak Ridge, TN 37831-6156 USA

James R. Keiser
Distinguished R&D Staff Member
Oak Ridge National Laboratory
Oak Ridge, TN 37831-6156 USA

ABSTRACT

There has been recent interest in exploring revolutionary supercritical CO_2 (sCO_2) cycles and a small effort is exploring what materials may be compatible with CO_2 at up to 1200°C. Initial exposures were conducted at 1 and 20 bar CO_2 for 1000 h at 1000° and 1200°C. As expected, Mo and W specimens that might be used as matrix materials in cermets were rapidly attacked under these conditions. Even alumina-forming FeCrAl alloys showed high mass gains in less than 100 h at 1200°C and 500 h at 1000°C due to the formation of Fe-rich oxide. Both Fe- and Ni-based alloys exposed at 1000°C showed higher mass gains than formed in air. Thus, Ni-based alloys appear compatible with sCO_2 up to 800°C but less so at higher temperatures. Low mass gains were observed for CVD SiC but $MoSi_2$ and MoSiAl specimens did not form protective scales under these conditions.

INTRODUCTION

Supercritical CO_2 (sCO_2) has several unique properties such as its low critical point (31°C/73.8 bar) that make it attractive for a number of different power generation applications including nuclear, fossil, concentrating solar power (CSP), geothermal and waste heat recovery [e.g. Dostal 2006, Chen 2010, Allam 2013, Iverson 2013, Wright 2013, Cheang 2015]. While some near-term applications have <550°C temperatures, fossil and CSP applications are interested in applications >700°C to enable >50% system efficiency [Feher 1968]. Several recent studies have determined that Ni-based structural alloys are compatible with sCO_2 at temperatures up to 800°C [Lee 2015, Olivares 2015, 2018, Oleksak 2018, Pint 2019, 2020]. Particularly, precipitation strengthened or age hardened Ni-based alloys such as Inconel 740H [Zhao 2003, Shingledecker 2013] and Haynes 282 [Pike 2008] enable sCO_2 cycle designs at 700°-800°C. However, the mechanical properties of these alloys drop significantly in this temperature range [Viswanathan 2005] and their ASME code cases (recently approved for alloy 282) limit their maximum use temperature to 850°-875°C. Attracted by increased efficiency goals, even higher temperatures would make sCO_2 cycles more attractive for development in new applications and for replacing current technology such as the steam Rankine cycle.

Previously, oxide dispersion strengthened (ODS) FeCrAl alloys were evaluated for higher temperature applications (900°-1100°C) including the fabrication of a prototypical ODS FeCrAl heat exchanger for 1100°C operation in the UK in the 1990s using alloy ODM751 [Starr 1994]. However, issues with cost, joining and the supply chain have remained as impediments for ODS alloys. More recently, ceramic matrix composites (CMC)[e.g. Naslain 2004] and cermets (ceramic-

metal composites) [e.g. Dickerson 2002, Grzesik 2003, Caccia 2018] have attracted more attention for gas turbine components and very high temperature (1200°-1400°C) applications.

The objective of this project was to explore the performance of potential candidate alloys at 1000°-1200°C in sCO_2 as very little prior work has been conducted at such a high temperature [Wright 2004, Oh 2006, Moore 2012, Pint 2017a]. Unfortunately, the current ORNL autoclaves are not capable of such high temperatures at supercritical pressures [Pint 2015, 2017b]. Thus, the experiments were conducted at 1 and 20 bar to evaluate the performance of several candidate materials to guide future efforts such as selecting matrix materials for cermets [Peng 2019]. Unlike 700°-800°C, where Ni-based alloys performed similarly in air and sCO_2 [Pint 2020], these results suggest that CO_2 is a more aggressive environment for most conventional materials at 1000° and 1200°C and that higher pressure might further accelerate the degradation.

EXPERIMENTAL PROCEDURE

The chemical compositions of the structural materials studied are shown in Table 1. Alloy coupons (~12 x 20 x 1.5 mm) were polished to a 600 grit finish and ultrasonically cleaned in acetone and methanol prior to exposure. In some cases, three specimens of each material were exposed in each condition. Exposures were conducted for 20-500 h in the "Keiser" test rig [More 2000, Terrani 2014, Pint 2018] with parallel Hexoloy (SiC) containment tubes and the specimens held on a vertical alumina tube using alumina rods through holes in the coupons. The specimens were slowly heated to temperature in argon and then exposed to the same 99.995% purity, research grade (RG) CO_2 gas (typical vendor measured H_2O content of 4.1±0.7 ppm) with one tube at 1 bar and the second at 20 bar.

The specimen mass change was measured using a Mettler Toledo model XP205 balance with an accuracy of ±0.04 mg or ~0.01 mg/cm^2. After exposure, samples were metallographically cross sectioned in epoxy, in some cases with Cu plating to protect the reaction product. Reaction products were imaged using light microscopy and a field emission gun, scanning electron microscope (SEM) equipped with energy dispersive x-ray (EDX) analysis (TESCAN model MIRA3).

Table 1. Chemical composition of the alloys measured by inductively coupled plasma and combustion analyses in mass%.

Alloy	Fe	Ni	Cr	Al	Si	Other
APMT	69.0	0.12	21.6	4.9	0.53	2.8Mo,0.12Y,0.16Hf,0.10Zr,0.20Ta,0.049O
FeCrAlY	74.1	<0.01	20.6	5.3	<0.01	0.07Y
C26M	79.7		11.9	6.2	0.2	2.0Mo,0.03Y
ODS FeCrAl	83.5	0.01	9.7	6.0	0.02	0.2Ti,0.22Y,0.27Zr,0.11O,0.07C,0.02Mn
H214	3.5	75.9	16.0	4.3	0.08	0.2Mn,0.02Zr,0.01Ti,0.004Y
N693	4.8	62.1	28.6	3.1	0.05	0.2Mn,0.6Nb,0.4Ti,0.05Zr
713LC	0.03	74.2	12.1	6.2	0.01	4.5Mo,2.1Nb,0.7Ti,0.06Zr,0.07C
N738	0.03	60.8	16.5	3.7	0.01	8.6Co,1.7Mo,2.6W,1.8Ta,0.7Nb,3.4Ti,0.01Hf
M247	0.07	59.5	8.5	5.7	0.03	9.8Co,9.9W,0.7Mo,3.1Ta,1.0Ti,1.4Hf
CVD SiC		0.01			69.8	30.2C,0.003O
$MoSi_2$	0.14	<0.01		0.42	35.3	61.6Mo,2.3O,0.05Mg,0.02W,0.05C
$Mo(Si,Al)_2$	0.02	<0.01		12.0	19.8	67.6Mo,0.4O,0.04W,0.1C

RESULTS

Figure 1 shows the mass change results for the metal specimens exposed at 1200°C using 20- and 40-h thermal cycles. Mo and W specimens were exposed as potential cermet matrices. Similar to behavior in oxygen [e.g. Gulbransen 1960, 1963], both alloys were rapidly attacked in CO_2 with the mass loss due to MoO_3 or WO_3 evaporation somewhat larger at 20 bar compared to 1 bar. Surprisingly, the FeCrAl alloy specimens also showed higher mass gains than expected, particularly for the low Cr (10%) ODS FeCrAl [Dryepondt 2018], Figure 1. The mass gains for APMT and FeCrAlY of 3-5 mg/cm^2 after 100 h are small compared to the Mo and W specimens but a FeCrAlY alloy gained only 1.1 mg/cm^2 after 100 h in air [Pint 2003]. All of the metal specimens were removed after 100 h total exposure.

The ceramic specimens exposed for longer times at 1200°C are shown in Figure 2 with much smaller mass changes than those shown in Figure 1. These specimens also were exposed for 20- and 40-h cycles to 100 h but then were exposed for longer cycles for a total of 1000 hr. Slightly higher mass gains were observed on some SiC specimens (3 of CVD SiC and 3 of Hexoloy) at 20 bar CO_2. One $MoSi_2$ specimen was exposed in each condition. Specimens of quartz and fused silica also were exposed with very little mass change observed.

Figure 3 shows images of the FeCrAl APMT (Advanced Powder Metallurgy Tube) specimens after 20 and 40 h exposures. The scale thickness was much higher in 1 bar CO_2 (Figures 2a and 2c) compared to 20 bar CO_2 (Figures 2b, 2d and 2e). At 20 bar, the scale appeared to be fairly uniform (except for the oxide nodule shown in Figure 2d) but much thicker than would form in air after a similar exposure. After 40 hr, the average oxide thickness was ~20 μm at 20 bar and 106 μm at 1 bar. At 1 bar, the oxide appeared to include some internal oxidation and a non-uniform reaction front that increased from ~45 μm after 20 h to 106μm after 40 hr. Figure 4 shows SEM/EDS maps of the scales formed after 40 h at 1 and 20 bar. The scales appear to be largely Al_2O_3 although some Cr-rich oxide areas were noted for the thicker scale formed in 1 bar CO_2 and an outer Fe-

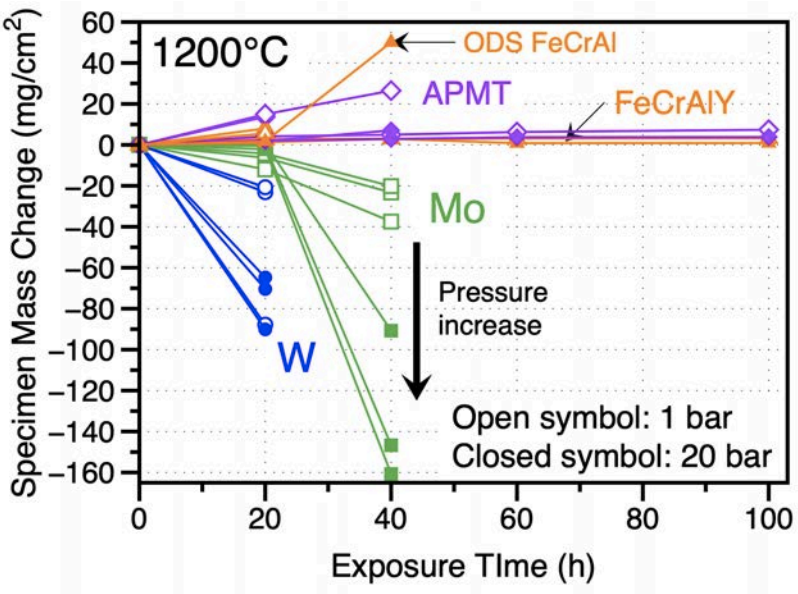

Figure 1. Specimen mass gain data for specimens exposed to RG CO_2 at 1200°C in 1 bar (open symbols) and 20 bar (closed symbols).

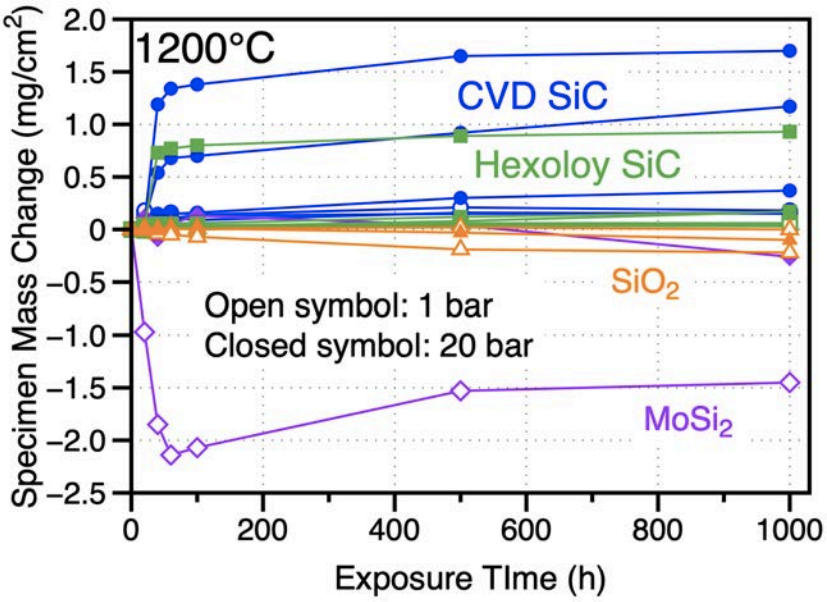

Figure 2. Specimen mass gain data for specimens exposed to RG CO_2 at 1200°C in 1 bar (open symbols) and 20 bar (closed symbols).

rich oxide layer formed after exposure in 20 bar CO_2.

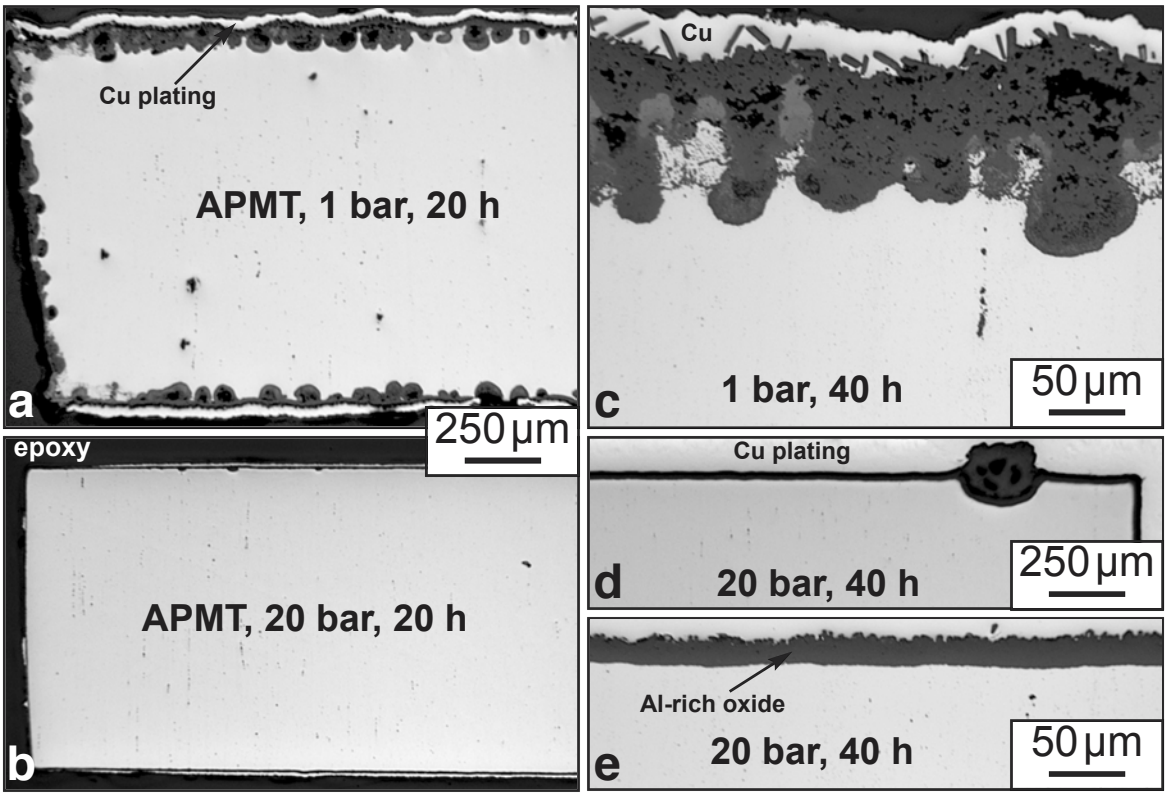

Figure 3. Light microscopy of APMT specimens exposed at 1200°C in 1 and 20 bar RG CO_2 (a) 1 bar, 20 h, (b) 20 bar, 20 h, (c) 1 bar, 40 h, (d,e) 20 bar 40 h.

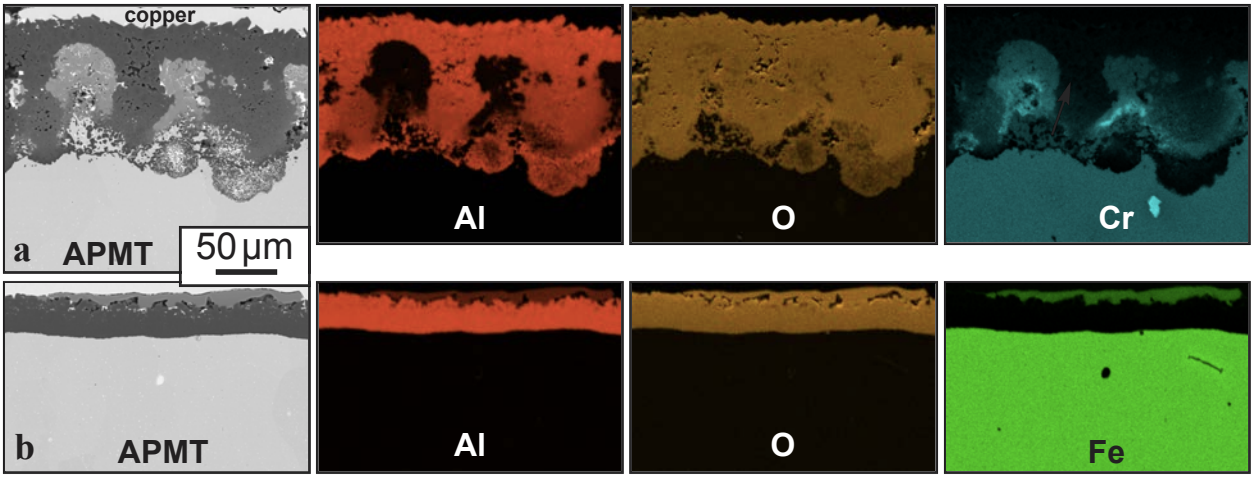

Figure 4: SEM analysis of APMT exposed for 40 h at 1200°C in (a) 1 bar and (b) 20 bar, with associated EDS maps.

Figures 5a and 5b show polished cross-sections of SiC specimens exposed for 1000 h in each condition. In some areas, a thicker reaction product was observed, Figure 5b. More characterization is needed to identify the composition and phase. However, the thin reaction product is consistent with the mass change in Figure 2.

For 1000°C exposures, Figure 6 shows mass change data for specimens exposed for 100 h in 1 and 20 bar CO_2. Similar to 1200°C, the Mo and W specimens showed large mass changes and the SiC specimens showed low mass changes in both 1 and 20 bar CO_2. Based on the positive results at 1200°C, additional $MoSi_2$ and $Mo(Si,Al)_2$ [Ingemarsson 2010] specimens were exposed at 1000°C. However, the mass gains were much higher than the SiC specimens, particularly for the $Mo(Si,Al)_2$ specimens exposed in 20 bar CO_2. The mass gains for the FeCrAl alloys were higher than expected as were the results for several Ni-based alloys tested. Figure 7 shows the mass change results for some of the metal specimens that were run for longer times with some specimens showing mass losses at longer times. To contrast these results, several specimens were oxidized for 1000 h (2, 500-h cycles) in laboratory air and those mass changes are compared to the CO_2 results in Figure 8. Increased mass gains in CO_2 ranged from 2-100X and several

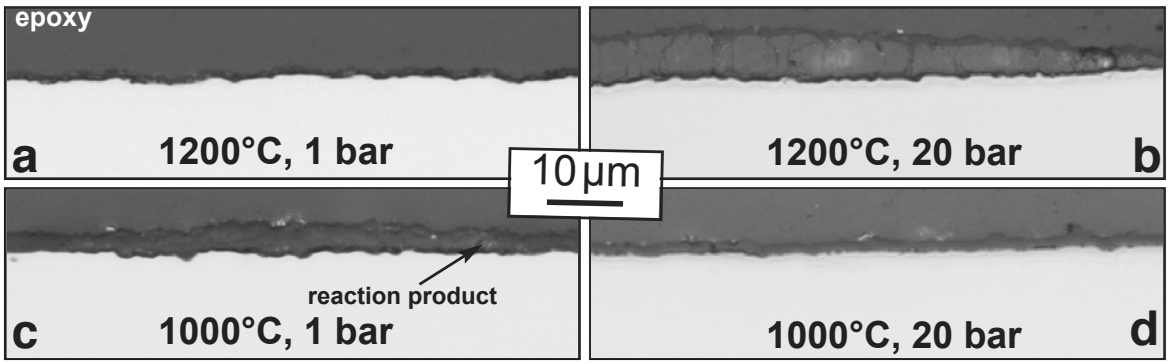

Figure 5. Light microscopy of CVD SiC specimens exposed for 1000 h at (a,b) 1200°C and (c,d) 1000°C in (a,c) 1 and (b,d) 20 bar RG CO_2.

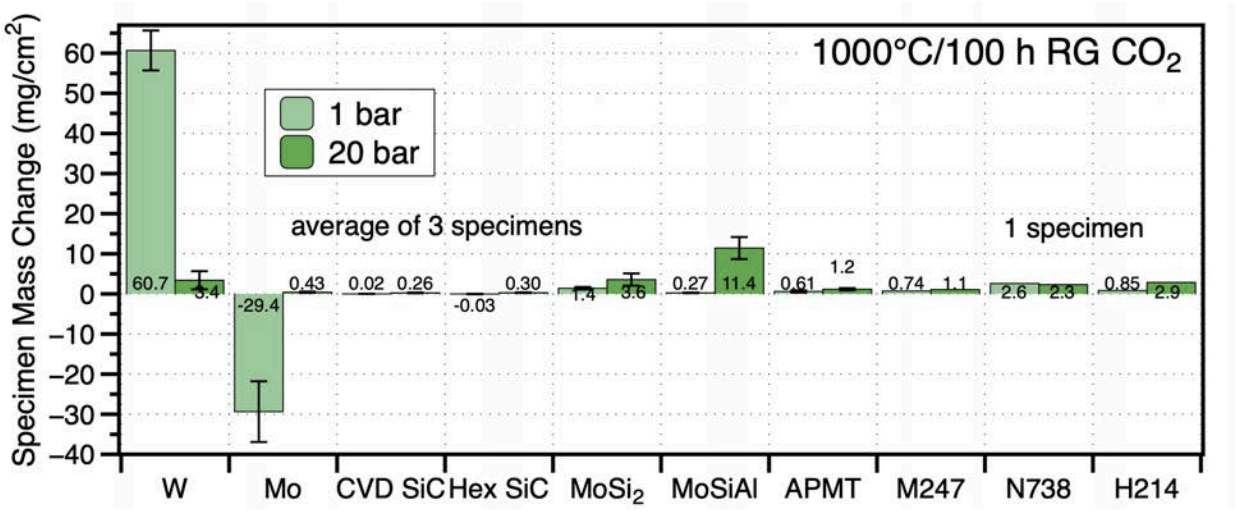

Figure 6. Specimen mass change after 100 h at 1000°C in RG CO_2 at 1 and 20 bar. The whiskers show a standard deviation and average values are shown except where noted.

specimens showed a mass loss after the 1 bar exposure and a large mass gain after the 20 bar exposure.

Figures 5c and 5d show the thin reaction products formed on CVD SiC after 1000 h at 1000°C in 1 and 20 bar CO_2, respectively. Figure 8 indicated that the mass gains in CO_2 were slightly higher than in laboratory air. For the metallic specimens, example reaction products are shown in Figures 9 and 10. In contrast to Figures 3 and 4 at 1200°C, the 20 bar condition appeared to result in thicker reaction products. In some cases, such as Figure 9c, the spallation of the reaction product

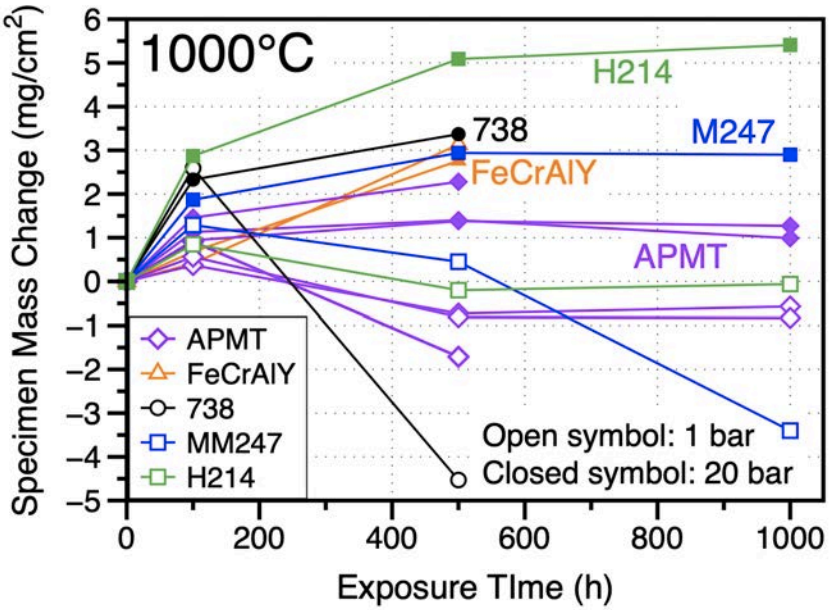

Figure 7. Specimen mass gain data for specimens exposed to RG CO_2 at 1000°C in 1 bar (open symbols) and 20 bar (closed symbols). Three APMT specimens were exposed in each conditon and one was removed after 500 h.

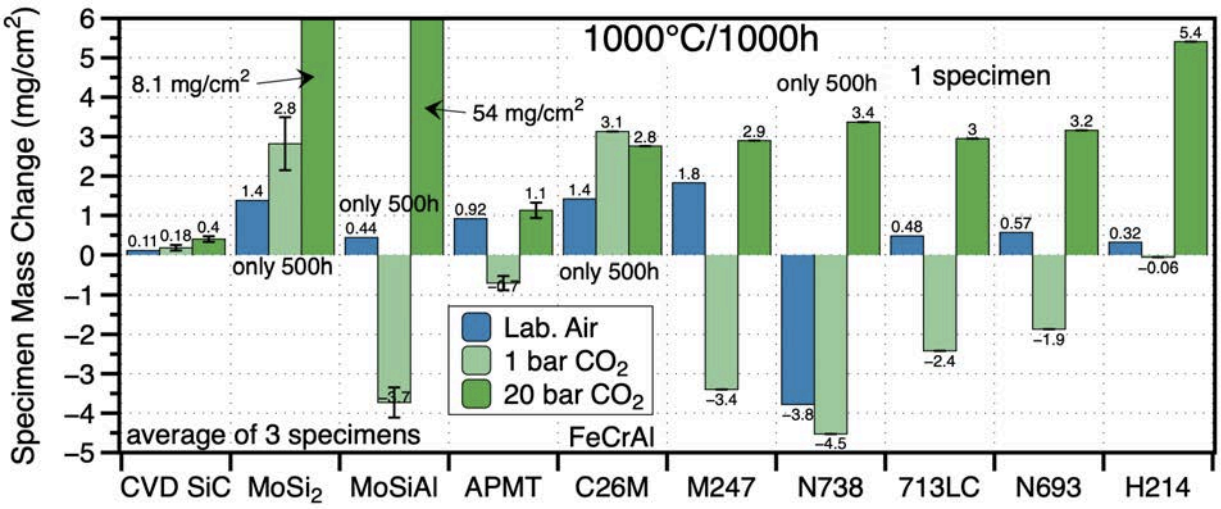

Figure 8. Specimen mass change after 1000 h at 1000°C in RG CO_2 at 1 and 20 bar compared to exposure in laboratory air. The whiskers show a standard deviation and average values are shown except where noted.

was consistent with the mass loss for the alloy N738 specimen, Figure 7. The internal oxidation observed indicated that the alloys were not able to exclusively form an Al-rich oxide under these conditions.

DISCUSSION

The results for the Mo and W specimens were as expected and suggest that a coating would be needed or other strategy utilized to protect W- or Mo-based cermets. Likewise, the CVD SiC, Hexoloy, quartz (crystalline) and fused silica (amorphous) specimens all showed low mass changes in most conditions at 1200°C suggesting that silica-forming alloys might do well in these environments. However, the $MoSi_2$ and $Mo(Si,Al)_2$ specimens showed higher mass gains than

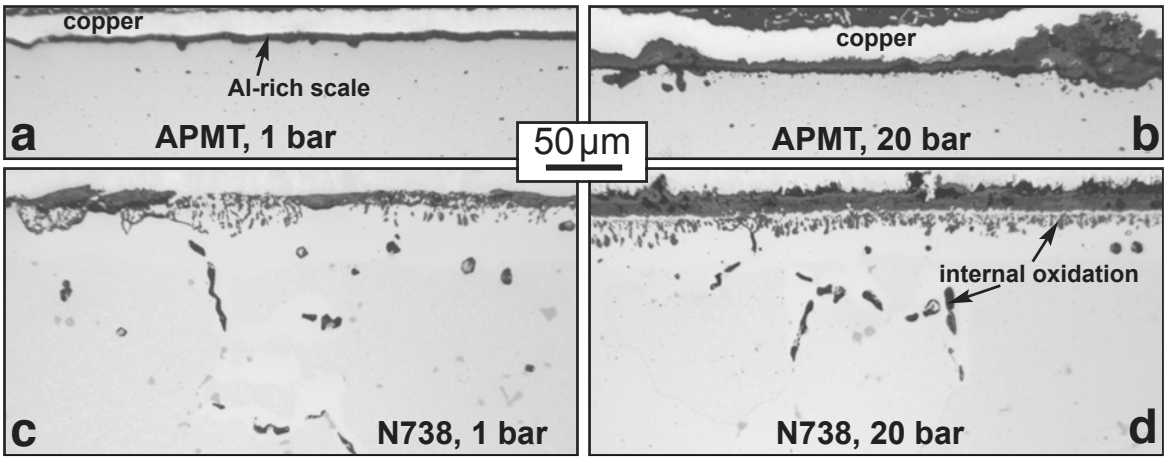

Figure 9. Light microscopy of (a,b) APMT and (c,d) N738 specimens exposed for 500 h at 1000°C at (a,c) 1 and (b,d) 20 bar RG CO_2.

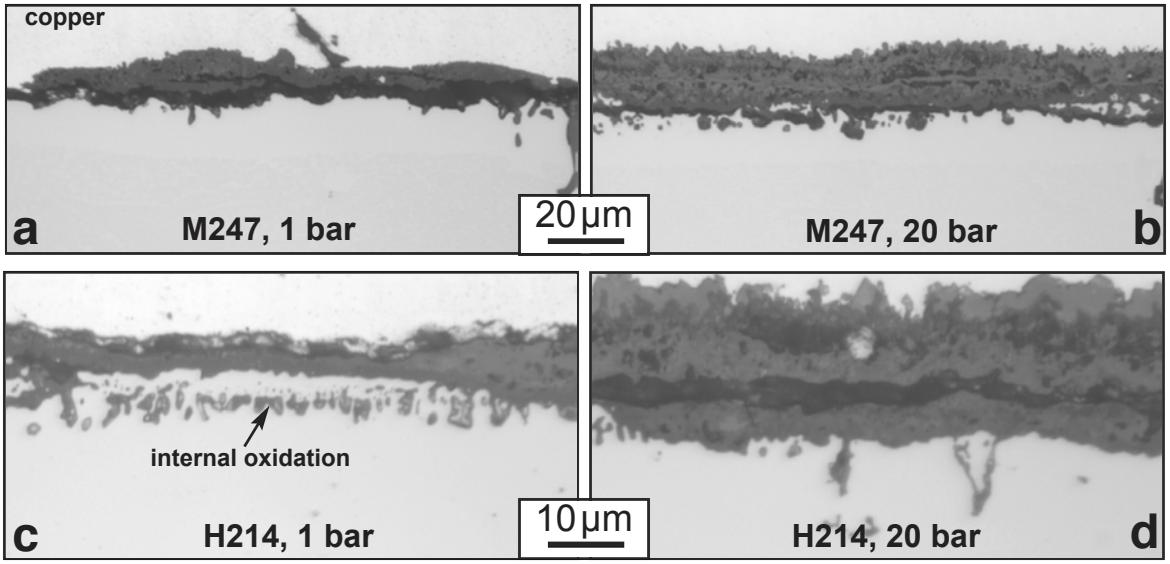

Figure 10. Light microscopy of (a,b) M247 and (c,d) H214 specimens exposed for 1,000 h at 1000°C at (a,c) 1 and (b,d) 20 bar RG CO_2.

expected at 1000°C. Characterization is still in progress to learn more about the reaction product formed on these alloys. For CVD SiC, Figure 5, the reaction products were thin but non-uniform and Figure 8 shows that the mass gains in CO_2 were higher than those observed in laboratory air.

APMT specimens were included as a surrogate for ODS FeCrAl. Alumina is considered to be less permeable to C than chromia scales [Jönsson 1997] so a more protective scale was expected to form under these conditions. However, there are few experiments where alumina-forming alloys have been exposed to CO_2 at ≥1000°C. An early study showed good resistance to carburization for type 406 stainless steel (Fe-12Cr-4Al) up to 982°C [McCoy 1965]. Another study used 10%CO_2-90%H_2O with exposures at 900° and 1135°C and observed mass gains higher than expected for similar exposures in air, but only limited characterization was performed [Wright 2004]. It has been known for many years that oxidation in CO_2 sets up a strong driving force for internal carburization [Gheno 2011, Gong 2017]. Recent work suggested that Ni-based alloys were less susceptible to internal carburization because of their lower C solubility [Olivares 2015]. After the FeCrAl alloys experienced higher than expected mass gains at 1200°C, several Ni-based alumina-forming alloys were included in the 1000°C experiment. However, all of the alloys experience higher mass gains than expected, Figures 6-8. The alumina-forming alloys such as APMT, 214 and M247 showed mass gains in air that were <1 mg/cm^2. For example, a 214 specimen gained 0.32 mg/cm^2 in two 500-h cycles in laboratory air at 1000°C. In 20 bar CO_2, the mass gain was <10X higher, Figures 7 and 8. In contrast, CVD SiC had a 0.11 mg/cm^2 mass gain in laboratory air at 1000°C, similar to the average mass gain of 0.18 mg/cm^2 in 1 bar CO_2, Figure 8. At 20 bar CO_2, the average mass gain was 0.40 mg/cm^2. Quantification of the reaction product thickness in Figure 5 is needed to better compare these results. In addition, thermodynamic calculations of the C activities in these environments will assist in understanding this behavior. Future work is in progress to expose cermet materials and explore the effect of pre-oxidation (e.g., to pre-form a protective Al-rich oxide in air) prior to CO_2 exposure. Initial results suggest limited benefit from this strategy.

SUMMARY

Initial exposures have been conducted for 1000 h at 1000° and 1200°C in RG CO_2 at 1 and 20 bar. As expected, cermet matrix materials like Mo and W were rapidly attacked under all conditions. CVD and Hexoloy SiC showed the most protective behavior and fused silica and quartz specimens exhibited only small mass changes, suggesting some promise for silica-forming materials and coatings under these conditions. However, $MoSi_2$ and $Mo(Si,Al)_2$ specimens showed higher mass gain than expected at 1000°C. The next round of testing is expected to include coated cermets and pre-oxidized candidate alloys to better understand the role of CO_2 at these extreme conditions.

NOMENCLATURE

CSP	=	Concentrated Solar Power
CVD	=	Chemical Vapor Deposition
ODS	=	Oxide Dispersion Strengthened
ORNL	=	Oak Ridge National Laboratory
RG	=	Research Grade

REFERENCES

Allam, R. J., Palmer, M. R., Brown Jr., G. W., Fetvedt, J., Freed, D., Nomoto, H., Itoh, M., Okita, N., Jones Jr., C., 2013, “High efficiency and low cost of electricity generation from fossil fuels while eliminating atmospheric emissions, including carbon dioxide,” Energy Procedia 37, 1135–1149.

Caccia, M., Tabandeh-Khorshid, M., Itskos, G., Strayer, A. R., Caldwell, A. S., Pidaparti, S., Singnisai, S., Rohskopf, A. D., Schroeder, A. M., Jarrahbashi, D., Kang, T., Sahoo, S., Kadasala, N. R., Marquez-Rossy, A., Anderson, M. H., Lara-Curzio, E., Ranjan, D., Henry, A. Sandhage, K. H., 2018, “Ceramic-metal composites for heat exchangers in concentrated solar power plants,” Nature 562, 406-409.

Cheang, V., Hedderwick, R. A, McGregor, C., 2015, “Benchmarking supercritical carbon dioxide cycles against steam Rankine cycles for Concentrated Solar Power,” Solar Energy, 113, 199-211.

Chen, H., Goswami, D. Y., Stefanakos, E. K., 2010, “A review of thermodynamic cycles and working fluids for the conversion of low-grade heat,” Renewable & Sustainable Energy Reviews 14, 3059-3067.

Dickerson, M. B., Snyder, R. L., Sandhage, K. H., 2002, “Dense, Near Net-Shaped, Carbide/Refractory Metal Composites at Modest Temperatures by the Displacive Compensation of Porosity (DCP) Method,” J. Am. Ceram. Soc., 85 (2002) 730–732.

Dostal, V., Hejzlar, P., Driscoll, M. J., 2006, “The supercritical carbon dioxide power cycle: Comparison to other advanced power cycles,” Nuclear Technology, 154(3), 283-301.

Dryepondt, S., Unocic, K. A., Hoelzer, D. T., Massey, C. P., Pint, B. A., 2018, “Development of low-Cr ODS FeCrAl alloys for accident-tolerant fuel cladding,” J. Nucl. Mater. 501, 59-71.

Feher, E. G., 1968, “The Supercritical Thermodynamic Power Cycle,” Energy Conversion, 8, 85-90.

Gheno, T., Monceau, D., Zhang, J., Young, D. J., 2011 “Carburisation of Ferritic Fe-Cr Alloys by

Low Carbon Activity Gases," Corrosion Science 53, 2767-2777.

Gong, Y., Young, D. J., Kontis, P. Chiu, Y. L., Larsson, H., Shin, A., Pearson, J. M., Moody, M. P., Reed, R. C., 2017, "On the breakaway oxidation of Fe9Cr1Mo steel in high pressure CO_2," Acta Materialia, 130, 361-374.

Grzesik, Z., Dickerson, M. B., K .H. Sandhage, K. H., 2003, "Incongruent reduction of tungsten carbide by a zirconium-copper melt," J. Mater. Research 18, 2135-2140.

Gulbransen, E. A., Andrew, K. F., 1960, "Kinetics of the Oxidation of Pure Tungsten from 500° to 1300°C", J. Electrochem. Soc. 107, 619-628.

Gulbransen, E. A., Andrew, K. F., Brassart, F. A., 1963, "Oxidation of Molybdenum 550° to 1700°C", J. Electrochem. Soc. 110, 952-959.

Ingemarsson, L., M. Halvarsson, J. Engkvist, T. Jonsson, K. Hellstrom, L. G. Johansson, J. E. Svensson, "Oxidation behavior of a $Mo(Si,Al)_2$-based composite at 300-1000°C," Intermetallics 18 (2010) 633-640.

Iverson, B. D., Conboy, T. M., Pasch, J. J., Kruizenga, A. M., 2013, "Supercritical CO_2 Brayton cycles for solar-thermal energy," Applied Energy, 111, 957-970.

Jönsson, B., Svedberg, C., 1997, "Limiting Factors for Fe-Cr-Al and NiCr in Controlled Industrial Atmospheres," Mater. Sci. Forum, 251-254 (1997) 551-558.

Lee, H. J., Kim, H., Kim, S. H., Jang, C., 2015, "Corrosion and carburization behavior of chromia-forming heat resistant alloys in a high-temperature supercritical-carbon dioxide environment," Corrosion Science 99 (2015) 227–239.

McCoy, H. E., 1965, "Type 304 Stainless Steel vs Flowing CO_2 at Atmospheric Pressure and 1100-1800°F," Corros., 21, 84-94.

Moore, R., Conboy, T., 2012, "Metal Corrosion in a Supercritical Carbon Dioxide – Liquid Sodium Power Cycle," Sandia National Laboratory Report SAND2012-0184.

More, K. L., Tortorelli, P. F., Ferber, M. K., Keiser, J. R., 2000, "Observations of Accelerated SiC Recession By Oxidation at High Water-Vapor Pressures," J. Am. Ceram. Soc., 83, 211-13.

Naslain, R., 2004, "Design, preparation and properties of non-oxide CMCs for application in engines and nuclear reactors: an overview," Composites Sci. Technol., 64 (2), 155-170.

Oh, C. H., Lillo, T., Windes, W., Totemeier, T., Ward, B., Moore, R., Barner, R., 2006, "Development Of A Supercritical Carbon Dioxide Brayton Cycle: Improving VHTR Efficiency And Testing Material Compatibility," Idaho National Laboratory Report INL/EXT-06-01271.

Oleksak, R. P., Tylczak, J. H., Carney, C. S., Holcomb, G. R., Dogan, O. N., 2018, "High-Temperature Oxidation of Commercial Alloys in Supercritical CO_2 and Related Power Cycle Environments," JOM 70, 1527-1534.

Olivares, R. I., Young, D. J., Marvig, P., Stein, W., 2015, "Alloys SS316 and Hastelloy-C276 in Supercritical CO_2 at High Temperature," Oxid. Met. 84, 585–606.

Olivares, R. I., Young, D. J., Nguyen, T. D., Marvig, P., 2018, "Resistance of High-Nickel, Heat-Resisting Alloys to Air and to Supercritical CO_2 at High Temperatures," Oxid. Met. 90, 1-25.

Peng, J., Lara-Curzio, E., Shin, D., 2019, "High-throughput thermodynamic screening of carbide/refractory metal cermets for ultra-high temperature applications," Calphad 66, 101631.

Pike, L. M., 2008, "Development of a Fabricable Gamma-Prime (γ') Strengthened Superalloy," in

Superalloys 2008, R. C. Reed et al. eds TMS, Warrendale, PA, 2008, p.191-200.

Pint, B. A., 2003, "Optimization of Reactive Element Additions to Improve Oxidation Performance of Alumina-Forming Alloys," J. Am. Ceram. Soc. 86, 686-695.

Pint B. A., Keiser, J. R., 2015, “Initial Assessment of Ni-Base Alloy Performance in 0.1 MPa and Supercritical CO_2,” JOM 67(11), 2615-2620.

Pint B. A., Brese, R. G., 2017a “High-Temperature Materials,” in Fundamentals and Applications of Supercritical Carbon Dioxide Based Power Cycles, K. Brun and P. Friedman, eds., Elsevier, London, pp.67-104.

Pint, B. A., Brese, R. G., Keiser, J. R., 2017b, “Effect of Pressure on Supercritical CO_2 Compatibility of Structural Alloys at 750°C,” Materials and Corrosion, 68, 151-158.

Pint, B. A., Brese, R. G., Keiser, J. R., 2018, “The effect of impurities and pressure on oxidation in CO_2 at 700°-800°C,” NACE Paper C2018-11199, Houston, TX, presented at NACE Corrosion 2018, Phoenix, AZ.

Pint, B. A., J. Lehmusto, J., Lance M. J., Keiser, J. R., 2019, “The Effect of Pressure and Impurities on Oxidation in Supercritical CO_2,” Materials and Corrosion, 70, 1400-1409.

Pint, B. A., Pillai, R., Lance M. J., Keiser, J. R., 2020, “Effect of Pressure and Thermal Cycling on Long-Term Oxidation in CO_2 and Supercritical CO_2” Oxidation of Metals 94, 505–526.

Shingledecker, J. P., Pharr, G. M., 2013, “Testing and Analysis of Full-Scale Creep-Rupture Experiments on Inconel Alloy 740 Cold-Formed Tubing,” J. Mater. Eng. Performance, 22, 454-462.

Starr, F., White, A. R., Kazimierzak, B., 1994, “Pressurized Heat Exchangers for 1100°C Operation Using ODS Alloys,” in: Materials for Advanced Power Engineering 1994, Eds. D. Coutsouradis, et al.; Kluwer Academic Publishers, Dordrecht, pp. 1393-1412.

Terrani, K. A., Pint, B. A., Parish, C. M., Silva, C. M., Snead, L. L., Katoh, Y., 2014, “Silicon Carbide Oxidation in Steam up to 2 MPa,” J. Am. Ceram. Soc. 97, 2331-2352.

Viswanathan, R., Henry, J.F., Tanzosh, J., Stanko, G., Shingledecker, J., Vitalis, B., Purgert, R., 2005, “U.S. Program on Materials Technology for Ultra-Supercritical Coal Power Plants,” J. Mater. Eng. Performance 14(3), 281-285.

Wright, I. G., Pint, B. A., Zhang, Y., Bishop, R. A., Farmer, J. C., Jankowski, A., Rebak, R. B., 2004, “Preliminary High-temperature oxidation data in steam-CO_2 in Support of the ZEST Process,” NACE Paper 04-531, Houston, TX, presented at NACE Corrosion 2004, New Orleans, LA, March 2004.

Wright, I. G., Pint, B. A., Shingledecker, J. P., Thimsen, D., 2013, “Materials Considerations for Supercritical CO_2 Turbine Cycles,” ASME Paper #GT2013-94941, presented at the International Gas Turbine & Aeroengine Congress & Exhibition, San Antonio, TX, June, 3-7, 2013.

Zhao, S. Q., Xie, X. S., Smith, G. D. Patel, S. J., 2003, “Microstructural stability and mechanical properties of a new nickel based superalloy,” Mater. Sci. Eng. A 355, 96-105.

ACKNOWLEDGMENTS

The authors would like to thank M. Howell, B. Johnston, T. Lowe, T. Geer and V. Cox for assistance with the experimental work. E. Lara-Curzio and K. Kane provided helpful comments on the

manuscript. This research was sponsored by the U.S. Department of Energy, Office of Fossil Energy, Crosscutting Technology Program. This manuscript has been authored by UT-Battelle, LLC under Contract No. DE-AC05-00OR22725 with the U.S. Department of Energy.